Silver photochemical reactivity under electronic irradiation of zinc-phosphate and sodium gallo-phosphate glasses

Fouad Alassani, Jean Charles Desmoulin, Olivier Cavani, Yannick Petit, Thierry Cardinal, Nadège Ollier

Silver Photochemical reactivity under electronic irradiation of Zinc-Phosphate and Sodium Gallo-Phosphate glasses

Fouad Alassani,[1] Jean Charles Desmoulin[1], Olivier Cavani[2], Yannick Petit[1,3] , Thierry Cardinal[1], Nadège Ollier[2]

[1]*Université de Bordeaux, CNRS, Bordeaux INP, ICMCB, UPR 9048, F-33600 Pessac, France*
[2] *Laboratoire des Solides Irradiés, UMR 7642 CEA-CNRS-Ecole Polytechnique, Palaiseau, France*
[3]*Université de Bordeaux, CNRS, CELIA, UMR 5107, 33405 Talence Cedex, France*

Corresponding author : fouad.alassani@u-bordeaux.fr

Abstract

In the present work, the effect of electron irradiations on silver-containing phosphate glasses using a 2.5 MeV electron beam has been explored by Electron Spin Resonance (ESR) and luminescence spectroscopy. The process involved in the interaction of electron beam with both the silver-containing and silver-free phosphate glass matrix and the formation of colored centers is discussed. This allowed an understanding of the initial phenomena of electron deposition and charge trapping that supports the photosensitivity of these glasses by identifying the point defects and the Ag species. The effect of the silver concentration and the structure of the glass depending on the integrated dose have been investigated. The in-situ cathodoluminescence measurements give additional valuable information about the cascade of chemical reactions in the formation of new silver species, namely from the initial silver ions to the molecular silver clusters.

Keywords: Silver containing Phosphate glass, Silver photochemistry, electronic irradiation, Color centers, silver clusters.

1 Introduction

Phosphate glass is considered to be a very promising material for high-performance optics as well as laser engineering applications because of its simple synthesis, low transition temperature, easy drawing, and large solubility of numerous transition metals or Rare Earths [1]. Recently the Direct femtosecond Laser Writing (DLW) technique has received great attention for its ability to integrate photonic devices within the diffraction limit in transparent photosensitive dielectrics and in particular in silver-containing phosphate glasses. Indeed, in silver-containing phosphate glass, femtosecond infrared DLW at a high repeating rate (MHz) and low laser power (few nanojoules) can initiate the photochemistry of the silver ions through multiphoton ionization to form molecular silver clusters (Ag_m^{x+}) with less than 10 silver atoms [2–5]. The generated silver clusters were believed to be responsible for the change in local properties of the glass, such as the induced local fluorescence [6–9] the second and third harmonic generation [10–12], the plasmonic resonance [4,13], and the localized refractive index change [14,15]. Recently, we have reported the influences of the glass sodium gallium

phosphate composition under DLW fs in the Na_2O-P_2O_5-Ga_2O_3 system [8]. Phosphate glasses are made up of polymer chains of PO_4 phosphate tetrahedron Q^n units, in which n is the number of bridging oxygen [16, 17]. As a function of the oxygen to phosphorus ratio, different associations of Q^n units are obtained [8]. The photosensitivity of silver containing polyphosphate and orthophosphate has recently been investigated [8, 18]. It was revealed that the orthophosphate exhibits high photosensitivity and larger silver cluster formation under DLW fs compared to the polyphosphate [8]. However, the understanding of the photochemical phenomena allowing the formation of the silver clusters, which are at the origin of the fluorescence in the phosphate glass remains unclear. Femtosecond laser interaction with glass creates highly out-of-equilibrium free electrons that allow for the activation of silver-based photo-chemistry and associated local material modifications at the root of high optical contrasts both for linear and nonlinear optical properties, but the limited volume of the voxel of interaction does not allow deploying the classical spectroscopy techniques such asESR for identifying the different paramagnetic species formed. In this framework, it is highly interesting to perform high-energy ionizing irradiation i.e. 2.5 MeV electrons to access the initial mechanisms of material modification, and thus to provide the fundamental understanding of the material parameters that play a role in the electrons and holes trap formation. Indeed interaction with an electron beam using high electron energy provokes a cascade of electrons resulting in the generation of high density of free electrons and holes within the glass matrices comparable to the case of femtosecond laser. Such phenomenon occurring in the whole volume of glass sample allows identifying by ESR, absorption, or luminescence spectroscopies, for instance, the resulting defects on the matrix or on silver ions and the formation of novel induced species**.** Still one has to keep in mind when establishing comparison that both femtosecond laser and electron irradiation lead to different kinetic, dose, and temperature.

Thanks to the formation of silver based electron and hole traps, silver containing phosphate glass have received much attention for dosimetry applications. Indeed, under the ionizing irradiation of the silver-containing phosphate glass, electron-hole pairs are generated. These electron-hole pairs are then trapped either directly or indirectly by transfer of the colored centers to the Ag^+ ions to form Ag^0 and Ag^{2+} leading to characteristic luminescence properties [19–21]. Due to the presence of an unpair electron on their $4d^9$ and $4d^{10}5s^1$ electronic configurations respectively, Ag^0 and Ag^{2+} are referred to as paramagnetic centers. The mechanism of the formation of the paramagnetic center in silver-doped phosphate glass has been widely reported using optical and electron spin spectroscopy (ESR) [19, 20, 22, 23].

In this paper, we report the use of electron 2.5 MeV irradiation with SIRUS accelerator on samples of silver-containing phosphate glasses. The aim is to assess the influence of the electron beam on the generation of defects and luminescent centers. ESR spectroscopy was carried out to determine the paramagnetic centers that were formed during the irradiation and the influence of the irradiation dose. In addition, the effect of the silver concentration as well as the effect of the structure of the phosphate glass network on the formation of the different species has been carried out. Time-resolved cathodoluminescence spectroscopy was also conducted to investigate the mechanism of formation of the silver centers in situ from the initial step of electron-hole pair formation.

2 Materials and methods

2.1 Glass synthesis

The silver-containing gallium zinc phosphate ($PZnGa_{5.5}$:Ag) and sodium gallo phosphate glasses (GPN:Ag) with the composition listed in Table 1 have been prepared from the following precursors: H_3PO_4 (Roth, 85%), Na_2CO_3 (Alfa Aesar, 99.95%), Ga_2O_3 (Strem Chemicals, 99.998%) and $AgNO_3$ (Alfa Aesar, 99.995%), ZnO (Fox chemical 99.99%). The precursors were then mixed in an aqueous solution in a Teflon beaker and dried over a sand bath for 12 hours to produce the cement. The cement was ground and placed into a platinum crucible and dried at 900°C for 1 hour to eliminate the residual carbonate and nitrate compounds. The dried cement was melted at 1050°C for both PZn and GPN_p and 1400°C for GPN_o for 24 hours with an intermediate quench and grind to maximize the homogenization of the Ag^+ silver ions. Finally, the glasses were quenched at room temperature and then annealed at 30°C below the glass transition temperature (Tg) for 4 hours to reduce the mechanical stress. The annealed glasses were subsequently cut into small pieces and optically polished on the two parallel faces.

2.2 Sample irradiation and cathodoluminescence

Glass samples of 4 mm x 5 mm x 0.7 mm were continuously irradiated at LSI (Laboratoire des Solides Irradiés), Palaiseau, France, and supported by the French Network EMIR using the SIRIUS electron accelerator with an electron beam size of 7 mm diameter. The electron energy is 2.5 MeV in order to homogenously irradiate glass samples of 0.7 mm thick at 10^4 Gy and 10^6 Gy. The sample holder was kept at room temperature with a water cooling system. The emission from the front face of the sample is collected at 45° (angle between the electron beam and collecting fiber) through a lens associated with the detection fiber. The detection fiber is 14 meters long and can reach the spectrometer and ICCD camera that is located in another room than the irradiation for security reasons.

2.3 Sample characterization

ESR spectroscopy was carried out to analyze the paramagnetic point defects formed during the electron beam exposure. JOEL JESX310, an X-band (9.8 GHz) spectrometer was therefore used at room temperature. The power of the microwaves was optimized for each defect to work in unsaturated conditions.

A Cary 5000 Spectrometer (Varian) was used for collecting the UV-Visible transmission spectrum.

The SPEXFluorolog-3 spectrofluorimeter (Horiba Jobin-Yvon) is used to monitor the photoluminescent properties (excitation and emission) of the irradiated glass at room temperatures. The setup is provided with a 450 W Xenon lamp and a Hamamatsu R298 photomultiplier. The emissions were recorded at room temperature with an Edinburgh Analytical Instruments M300 monochromator, a Xe-900 lamp and an AMHERST SCIENTIFIC CORP. 4100 cooled PMT

3 Results and discussion

3.1 Glass composition and properties

Unlike silica Glass, phosphate glass presents more advantages such as low melting temperature and the ability to contain high amounts of transition ions such as silver. Glasses in two glass systems have been investigated: Zinc phosphate and sodium gallo phosphate. Zinc phosphate

glass ($PZnGa_{5.5}$) for instance with oxygen to a phosphorous ratio greater than 3.25 exhibits good stability toward direct femtosecond laser writing with the formation of colored centers [24, 25]. Such a matrix allows the solubility of a large concentration of silver clusters. In the past two decades, we have demonstrated the role of silver ions as a photosensitive agent in zinc phosphate glasses [26] and their ability to undergo photochemical reactions to form luminescent silver clusters under femtosecond laser writing [9]. Thus, in this paper, zinc phosphate glasses as illustrated in Table1 have been chosen to investigate the effect of the silver concentration on the formation of colored centers following electronic irradiation. A 5.5 cationic percent of gallium has been introduced into the glass composition to stabilize the glass network toward moisture. For the same $PZnGa_{5.5}$ glass composition (pyrophosphate), the cationic percentage of silver varied from 0 to 8 %. All $PZnGa_{5.5}$ glasses presented UV-blue homogenous fluorescence (not shown here) under a 254 nm UV lamp, which is the signature of good dispersion of silver ions within the glass matrix without detrimental reduction effect [27, 28]. The increasing silver content influences the physical-chemical property of the phosphate glass by the formation of non-bridging oxygens which decrease the glass transition temperature. Indeed the presence of Ag_2O in phosphate glass tends to break the P-O-P bond inducing the depolymerization of the glass network and lowering the covalence character of the phosphate glass skeleton. To investigate the glass structure impact on the formation of paramagnetic centers, three glass compositions have been selected with the same number of silver ions per cm^3. Sodium-gallo pyrophosphate and orthophosphate glasses in the glass system Na_2O-P_2O_5-Ga_2O_3 labeled GPN_p and GPN_o respectively, as well as $PZnGa_{5.5}$ pyrophosphate, have been targeted. The GPN_o without silver was also synthesized to well illustrate the effect of the presence of silver. Regarding the GPN_p composition, a silver-free glass with good optical quality could not be obtained. In the case of the sodium gallo phosphate glass as for pyrophosphate, one can notice that introducing a modifier such as silver and sodium tends to decrease the glass transition temperature.

Acronym	Cationic composition					NAg^+ ($10^{-20}.cm^{-3}$)	Tg (±2°C)
	$PO_{5/2}$	$GaO_{3/2}$	$NaO_{1/2}$	ZnO	$AgO_{1/2}$		
$PZnGa_{5.5}$	56.0	5.5	-	38.5	0	0	435
$PZnGa_{5.5}$-$Ag_{1.5}$	55.1	5.5	-	37.9	1.5	3.9	422
$PZnGa_{5.5}$-$Ag_{3.0}$	54.2	5.5	-	37.3	3.0	8	410
$PZnGa_{5.5}$-$Ag_{5.5}$	52.7	5.5	-	36.3	5.5	13.6	396
$PZnGa_{5.5}$-$Ag_{8.0}$	51.3	5.4	-	35.3	8	22	381
GPN_p-Ag	56.0	28	14	-	2	5.7	497
GPN_o	31.58	21.05	47.37	-	0	0	399
GPN_o-Ag	31.0	20.6	46.4	-	2	6.5	385

Table 1: Cationic compositions of prepared glasses, the number of silver ions per volume (NAg^+), and the glasses' transition temperature (Tg).

3.2 Effect of silver content in $PZnGa_{5.5}$ glasses analyzed by ESR.

This section aims to understand the impact of the electron beam on silver-containing phosphate glass. Thus, $PZnGa_{5.5}$ glasses with various concentrations of silver (Table1) were irradiated with an electron beam using the NEC SIRUS electron accelerator. The irradiation energy and dose are 2.5 MeV and 10^6 Gy respectively. Subsequently, the irradiated samples were analyzed by ESR spectroscopy at room temperature for identifying the different paramagnetic centers formed during irradiation. Figure 1 depicts the ESR spectra of irradiated silver-doped and non-doped $PZnGa_{5.5}$ glasses. The ESR spectrum of the unirradiated glass (not shown here) did not reveal any ESR signal linked to any paramagnetic center. Thus, it is assumed that the silver ions

were well dispersed and fully oxidized to their Ag^{+} form with an electronic configuration of $4d^{10}$ and showed no unpaired electrons before irradiation. However, the ESR spectra of the irradiated glass exhibit many ESR signals linked to the existence of various paramagnetic defects that depend on the silver content. For the non-silver doped glass (blue curve), the saturated signal doublet located at 3493 Gauss and 3528 Gauss can be assigned to a hole center located on non-bridging oxygen bound to a phosphorus atom and named Phosphorus Oxygens Hole Center (POHC) [29, 30]. This doublet originates from the hyperfine splitting resulting from the interaction between the ½ nuclear spin of the phosphorus atom and the spin of the trapped hole. For the $PZnGa_{5.5}$:$Ag_{0.5}$ (green curve), the POHC defect contribution decreases dramatically (see inset of Figure 1) with the apparition of new signals. The signal at 3680 Gauss can be linked to one contribution of the doublet of PO_2^{2-} (P_4) defect [30, 31]. Indeed, the PO_2^{2-} defect is typically considered as an electron trap center with a characteristic doublet at A_{iso} = 305 Gauss in the ESR for phosphate glass [30]. The signals at 3000, 3200, 3400, and 3850 Gauss probably originate from the presence of silver and are associated with highly stable silver-related paramagnetic defects. The broad and main signal at 3000 Gauss and the intense signal at 3400 Gauss seen in all silver-doped glass can be ascribed to the hole trapped center of Ag^{2+} doublet [19, 21, 32]. With the increase of silver concentration to 3% and 5.5% in $PZnGa_{5.5}$ (Figure 1 red curve and black curve respectively), the intensity of the ESR signal of Ag^{2+} increases and almost reaches its maximum. The shifting of the ESR signal at 3400 Gauss for $PZnGa_{5.5}$:$Ag_{0.5}$ may result in the overlapping of the second contribution of PO_2^{2-} doublet and Ag^{2+} signals. While the ESR signals around 3200 and 3850 Gauss can be assigned to the silver's electron trapped center of (Ag^{0}) doublet [5, 9, 22, 33]. The increase in the intensity of the Ag^{0} signal with the increasing silver contents is also observed.

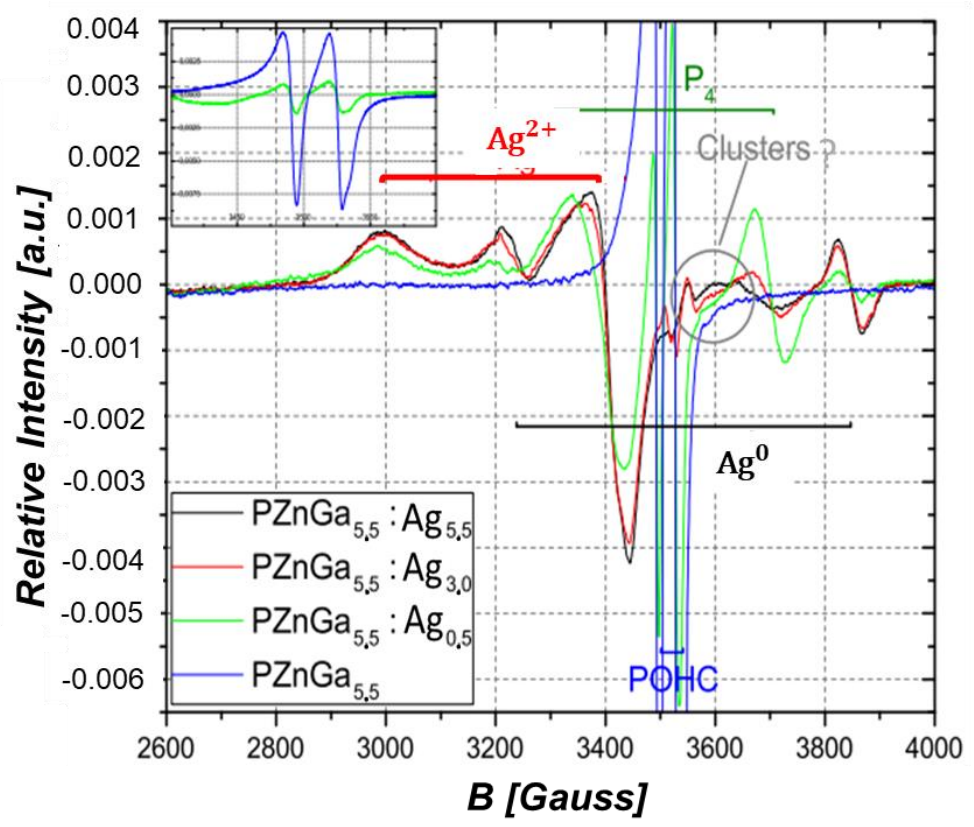

Figure 1: ESR spectra of electronic irradiated $PZnGa_{5.5}$: Ag_x glass with different concentrations of silver showing the signals of paramagnetic electron and hole trapped center formed (insect: signal of POHC defect).

To clarify the various processes related to the concentration of the defects induced by electron irradiation as a function of the silver doping concentration, semi-quantitative analysis was carried out by using the following equation $I \propto Y_{max} * (\Delta H_{pp})^2$. Where Y_{max} is the peak-to-peak amplitude of the signal and ΔH_{pp} is the width of the peak-to-peak of the related signal. As the magnitude of the ESR signals of each species depends on the silver ion concentration in the pristine glass and the induced defect concentration, this will give an approximated quantitative trend for each paramagnetic defect. Figure 2 plots the trend of the normalized magnitude of the individual paramagnetic defects function of the molar concentration of silver ions in the virgin glass. It can be observed that the silver-free glass shows signals only corresponding to the POHC defect. For $PZnGa_{5.5}:Ag_{0.5}$, the POHC signal decreases significantly, while the PO_2^{2-} signal reaches its maximum. In addition, the Ag^0 and Ag^{2+} species are formed at 30% and 90% of their maximum values respectively. For the higher silver concentration ($PZnGa_{5.5}:Ag_3$), a significant inversion of both Ag^0 and PO_2^{2-} populations are observed, where Ag^0 increases to 90% while PO_2^{2-} decreases to 30%. At this stage, the POHC signal is no more detected. In the glass with the highest concentration of silver ions ($PZnGa_{5.5}:Ag_{5.5}$), the PO_2^{2-}species is not detected while the Ag^0 species become the only electron trap center. This variation in the magnitude of the ESR signals highlights the efficient substitution of the silver ions for phosphorus as the main hole and electron traps forming Ag^{2+} and Ag^0 centers. Indeed, the fast decrease of the POHC can be caused by electron and hole recombination or hole transfer to Ag^+. Indeed, the hole transfer from POHC to Ag^+ has been already reported in the literature [21, 34, 35]. In conclusion, in the silver-containing $PZnGa_{5.5}$ glass, Ag^+ ions entrap electrons and holes according to the following equation (1) to form silver-colored centers that can last for several weeks and have a very low recombination rate [36].

$$Ag^+ + h^+ \rightarrow Ag^{2+}$$

$$Ag^+ + e^- \rightarrow Ag^0 \qquad (1)$$

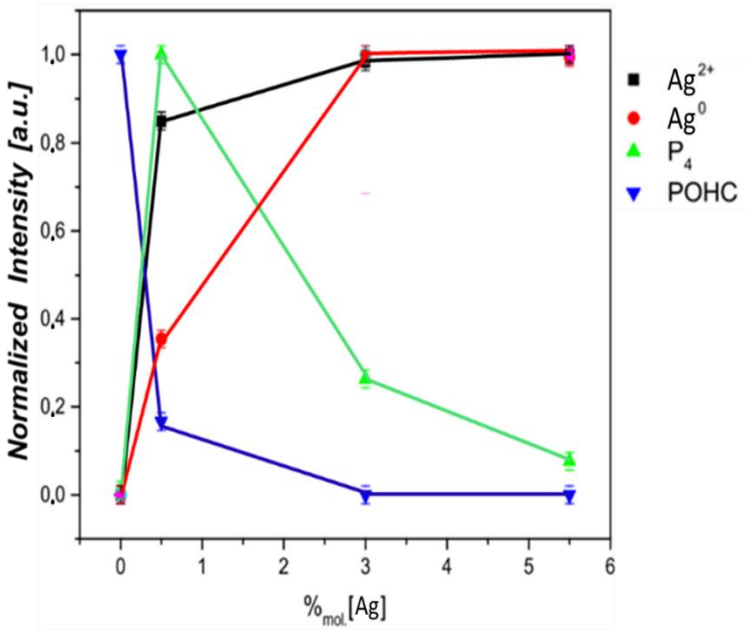

Figure 2: Trend of the evolution of the normalized ESR intensity of paramagnetic electrons and hole centers formed during electron irradiation of $PZnGa_{5.5}$ for different silver content

3.3 Effect of silver concentration on Absorption and luminescence properties $PZnGa_{5.5}$ glass

In this section, the absorption spectroscopy of the irradiated silver containing $PZnGa_{5.5}$ was performed to support the findings of ESR in the previous section. Figure 3 illustrates the absorption coefficient of $PZnGa_{5.5}$ glasses with different silver concentrations after electronic irradiation. For the silver-free $PZnGa_{5.5}$, the absorption spectrum (Figure 3 black curve) exhibits broadband up to the visible range with two contributions maximum at 540 nm (2.3 eV) and 410 nm (3.0 eV). These contributions can be associated with POHC defects [29]. From 300 nm to a lower wavelength in the UV range, a much more intense absorption is observed, which can be attributed to phosphate electron trap centers (EC) [29]. Once silver ions are added to $PZnGa_{5.5}$ glasses, new broad bands spanning from UV to visible range appeared (Figure 3 red curve). Those absorption bands are different from that of the undoped $PZnGa_{5.5}$ glass and their intensities increase with silver content exhibiting two maximum contributions around 280 nm and 380 nm. These two contributions can be associated with the formation of Ag^{2+} [18, 27, 37]. For the highest content of silver (Figure 3 green and blue curve), the band at around 280 nm shifts to the largest wavelength, and an additional contribution appears around 320 nm which can be associated with a new type of silver species. This finding is highly correlated to the ESR result presented in the previous section. The tail of the absorption band observed above 500 nm for the silver doped glass can be due to the defect centers, radiation damage, and diffusion phenomena.

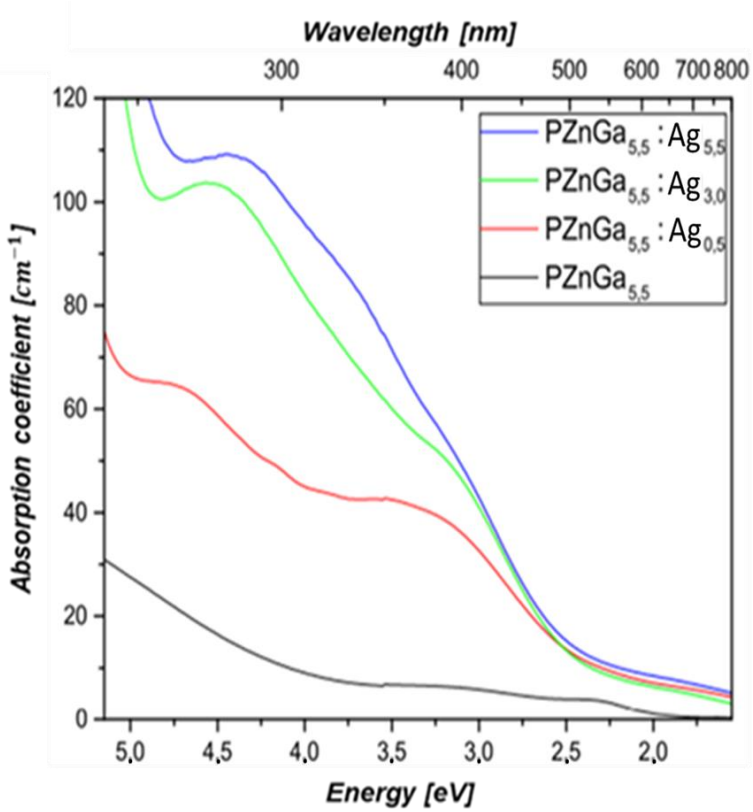

Figure 3: Absorption spectra of irradiated $PZnGa_{5.5}$: Ag_x for different silver concentration

To further investigate the silver species that are formed after electron irradiation, luminescence properties of irradiated silver containing $PZnGa_{5.5}$ were performed. Figure 4 illustrates the emission spectra for excitation at 305 nm and 380 nm and the excitation spectra for emission at

700 nm and 550 nm respectively. For $PZnGa_{5.5}:Ag_{0.5}$, the excitation at 305 nm induces a broad emission band with a maximum located around 525 nm and a shoulder located at 600 nm (Figure 4a full black curve). A similar band is seen for the glass containing a high concentration of silver ($PZnGa_{5.5}:Ag_3$ and $PZnGa_{5.5}:Ag_{5.5}$), the main peak, in this case, is located around 630 nm (Figure 4a full red curve and green curve respectively). For the emission spectra collected for excitation at 380 nm, the main peak around 525 nm with the highest intensity is seen in the glass with the highest silver content (Figure 4b full green curve), whereas the main peak at 630 nm with the highest intensity is seen in the glass with the lowest silver content (Figure 4b full black curve) indicating that different silver luminescent centers are formed upon electronic irradiation. To elucidate this finding, excitation spectra for emissions at 550 nm and 700 nm have been performed to identify the different contributions. For $PZnGa_{5.5}:Ag_{0.5}$ the excitation spectra for the two later emissions provide a broad signal with several contributions for which the identification of each contribution is quite ambiguous. For the emission at 700 nm one can distinguish an intense band below 300 nm and shoulder at 325 nm and 380 nm (Figure 4b dash black curve). For the excitation at 380 nm, the main band at 630 nm is associated to the silver Ag^{2+} as reported elsewhere by Bourhis *et al*., whereas the emission collected at 550 nm for the excitation at 305 nm is associated to silver clusters [9, 18, 37].

When the concentration of silver rises to 3% ($PZnGa_{5.5}:Ag_3$) and above (For $PZnGa_{5.5}:Ag_{5.5}$) the main emission bands for the two excitations at 305 nm and 380 nm are located at 500 nm and 630 nm (see full red and green curves in Figures 4a and 4b). For the emission of 700 nm, the collected excitation spectra (Figure 4a red and green dash curves) are characteristic of Ag^{2+} with maximum located at 280 nm, 320 nm, and 380 nm respectively [18, 27, 37]. However, the excitation spectra for the 550 nm emissions reveal an additional contribution at 355 nm (Figure 4b red and green dash curves) although such emission is characteristic of silver clusters with an excitation band with a maximum between 320 nm and 400 nm [18, 27, 37]. The luminescence spectroscopy evidence at least two cluster families for lower and higher silver concentration with maximum absorption respectively below 300 nm and between 300 - 400 nm.

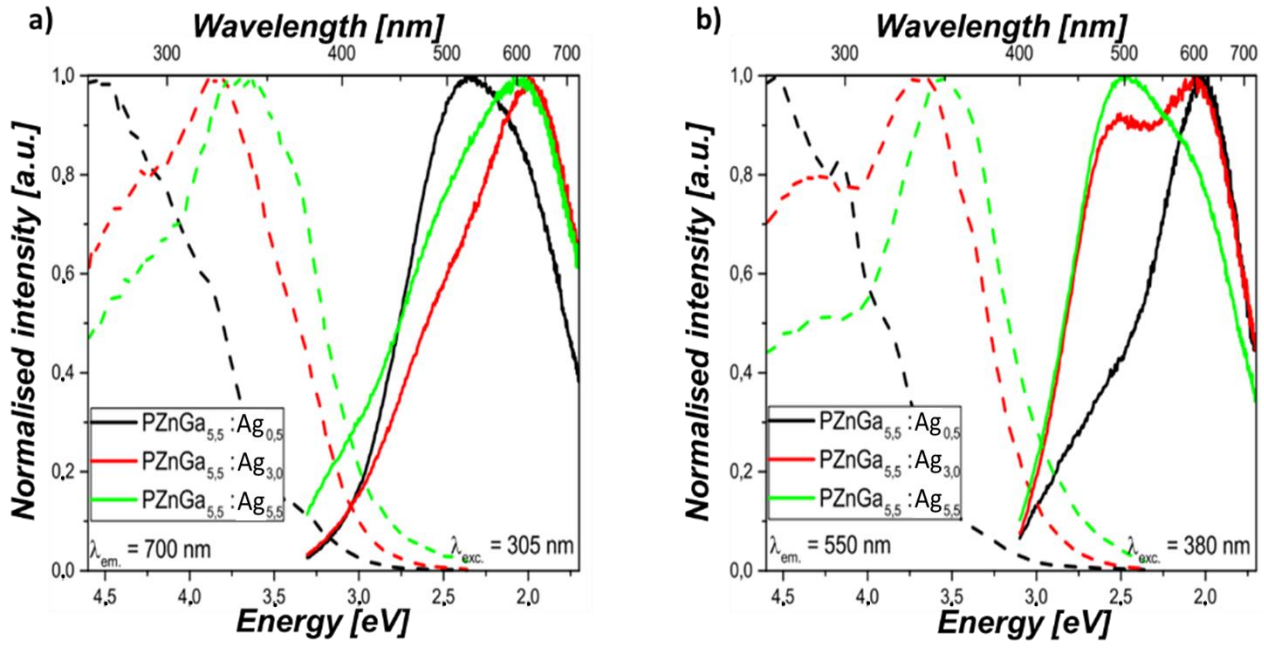

Figure 4: Photoluminescence properties of the irradiated $PZnGa_{5.5}:Ag_x$ glass, a) for 305nm excitation and 700 nm emission, b) for 380 nm excitation and 550 nm emission.

3.4 Influence of glass matrix analyzed by ESR

In this section, the interaction of the electron beam on the silver-containing glass is extended to phosphate glasses having a different network structure with a similar number of silver per cm^3 as the sample $PZnGa_{5.5}:Ag_3$. Ga_2O_3-P_2O_5-Na_2O glass system has been chosen to prepare optical quality silver containing pyrophosphate GPN_p and orthophosphate GPN_o (cf Table1). One can notice that GPN_p and $PZnGa_{5.5}$ exhibit both pyrophosphate structures with oxygen to phosphorus ratio [O/P] near 3.25.

Figures 5a and 5b depict the ESR spectra of GPN_p:Ag glasses irradiated at 10^4 Gy and 10^6 Gy respectively. The ESR signal of the 10^4 Gy irradiated glass shows a broad contribution at 2850 Gauss and a very intense contribution at 3200 Gauss that is attributed to the doublet of the trapped silver hole center (Ag^{2+}) [21, 22, 32]. Additional contributions around 3050 Gauss and 3630 Gauss associated with electron trap silver center's (Ag^0) doublet are also observed [5, 9, 22, 33]. These ESR signals of GPN_p:Ag at 10^4 Gy are quite comparable to that of $PZnGa_{5.5}:Ag_3$ irradiated at 10^6 Gy, meaning that the threshold to induce silver photochemical behavior is lower in GPN_p:Ag. When the irradiation dose increases to 10^6 Gy, the ESR signal of Ag^{2+} strongly increases relatively, compared to that of Ag^0. The behavior of Ag^0 signal amplitude is attributed to the simultaneous consumption of Ag^0 to form silver clusters as Ag^0 plays a key role in silver photochemistry reaction illustrated in the following equation.

$$aAg^0 + bAg^+ \dashrightarrow Ag_m^{x+} \text{ with } x = b \text{ and } m = a + b \qquad (2)$$

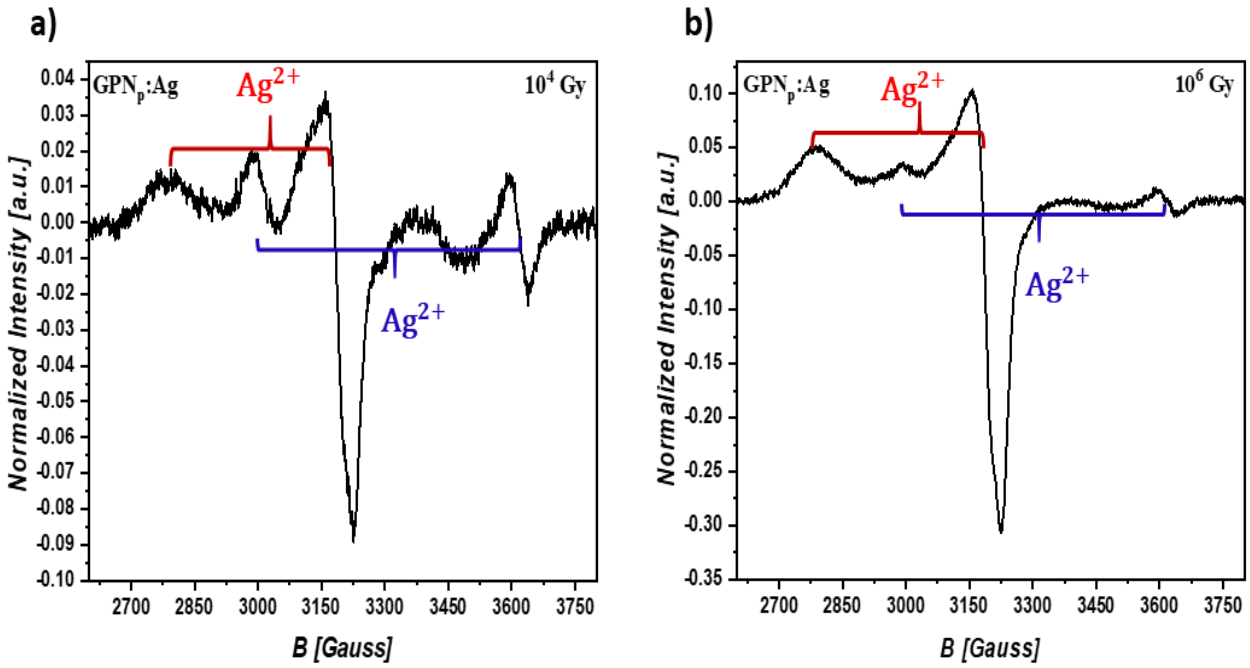

Figure 5: ESR spectra of irradiated GPN_p:Ag glass for two different radiation doses a) 10^4 Gy and b) 10^6 Gy.

Furthermore, the ESR spectrum performed on irradiated silver-containing and silver-free GPN_o at 10^4 Gy and 10^6 Gy is presented in Figure 6. For the silver-free GPN_o irradiated at 10^4 Gy the signal doublet observed around 3250 Gauss and 3300 Gauss (Figure 6a) is characteristic of phosphate oxygen hole center (POHC) defects [19, 22] as seen for $PZnGa_{5.5}$ (Figure 6 blue curve). In between the POHC doublet, two additional components are visible between 3280 Gauss and 3290 Gauss which may be linked to the radical peroxide II defect not detected in the

case of $PZnGa_{5.5}$ [30, 38]. Indeed, two bonded oxygen atoms linked to a phosphorus atom characterize the peroxide defect. Moreover, the shoulder around 3240 Gauss can be attributed to the radical peroxide I defect [30, 38]. For the 10^6 Gy dose, (Figure 6d) the radical peroxide defect intensity becomes higher while the intensity of the POHC defect decrease. This might be linked to the highest irradiation dose leading to a change in the host glass and promoting the P-O-O bond formation [30, 38]. One could assume the presence of a phosphate-related electrons center, which is barely invisible in this case. The phosphate-related electrons center's signal can be very weak and can be overwhelmed by the very intense signal of POHC. For GPN_o:Ag, the ESR spectra of the glasses irradiated at 10^4 Gy and 10^6 Gy, shown in Figures 6b and 6e respectively, revealed that the signal from the phosphate-related paramagnetic center vanishes altogether with the occurrence of new ones like in the case of $PZnGa_{5.5}$:Ag. The broad ESR signal at 2850 Gauss and the very intense signal at 3200 Gauss in the 10^4 Gy irradiated glass can be attributed to the doublet of Ag^{2+} [21, 22, 32]. Whereas the small broad signal between 3020-3100 Gauss is attributed to Ag^0 [5, 9, 22, 33]. By raising the dose to 10^6 Gy, only the Ag^{2+} ESR signal can be observed and the ESR signal of Ag^0 is not detected. Indeed, unlike pyrophosphate $PZnGa_{5.5}$:Ag and GPN_p:Ag glasses, the stabilization of Ag^0 in orthophosphate GPN_o:Ag glass is negligible, assuming that Ag^0 is rapidly consumed to form silver clusters. This reveals the higher photosensitivity of GPN_o:Ag compares to $PZnGa_{5.5}$:Ag and GPN_p:Ag upon ionizing irradiation [18]. It is therefore proposed that the variation of the ESR signal in both silver-containing and silver-free GPN_o as well as $PZnGa_{5.5}$ is correlated to the hole created by irradiation, initially being trapped on a shallow site of POHC and Peroxide, then transferred to Ag^+ to generate Ag^{2+} as shown in equation (1) in the case of silver containing glass. The broadband associated with the ESR signals of Ag^0 can result from electron transfer from a phosphorus-trapped center to Ag^+.

One can note that the emission spectra collected are in accordance with the luminescence spectroscopy previously reported in the case of femtosecond laser interaction validating the comparison of electron and femtosecond laser irradiation which lead both to the formation of silver traps and silver clusters. It also confirms that for large silver concentrations, both irradiations lead to the formation of silver species without affecting the phosphate glass skeleton. The process of silver trap and cluster formation under an electron beam, being dependent on the dose, allows also bringing some insight valuable to understand the silver species evolution and migration under femtosecond laser irradiation.

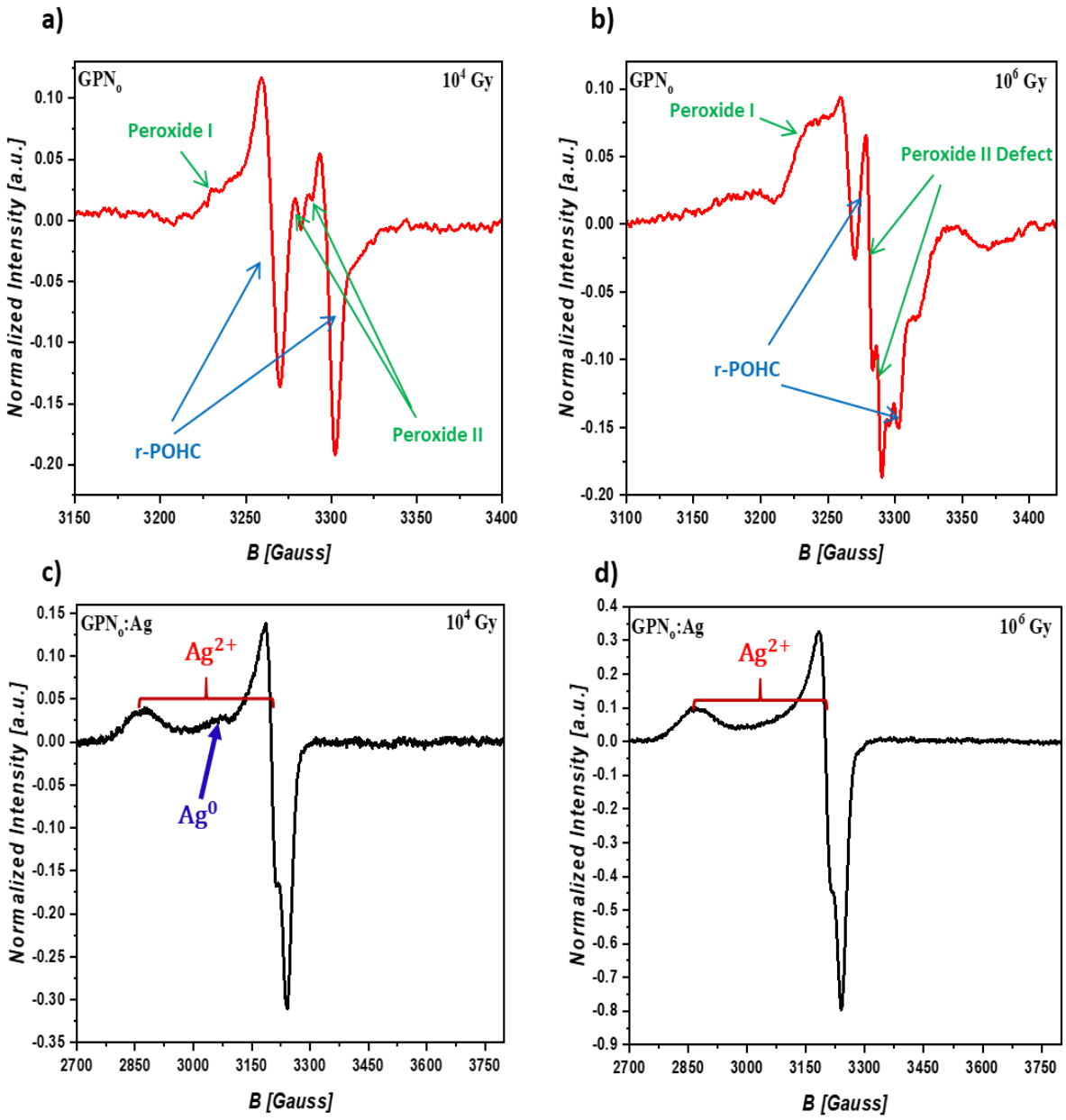

Figure 6: ESR spectra of Ag free and Ag containing GPN_o glass irradiated at 10^4 Gy and 10^6 Gy

3.5 Effect of the glass matrix structure on absorption and photoluminescence of irradiated GPN glasses

The absorption spectra of GPN_p:Ag and GPN_o:Ag irradiated at 10^4 Gy and their corresponding pristine glass is shown in Figure 7. The absorption edge of the pristine glasses is observed at below 280 nm and no further absorption bands are observed beyond 280 nm. This indicates that silver ions (Ag^+) are well dispersed and no clustering or plasmonic signature occurs. When the glasses are irradiated at 10^4 Gy, a wide absorption band covering the late UV with main contributions around 325 nm and 380 nm as well as a tail in the visible range can be observed in GPN_p:Ag (Figure 7a). Those absorption features are similar to the absorption collected on the 10^6 Gy irradiated $PZnGa_{5.5}$:Ag_3 glass. However, the GPN_o:Ag exhibits much more intense

absorption with the absorption edge shifting to the red compared to GPN_p:Ag. This is related to the formation of the largest amount of color centers.

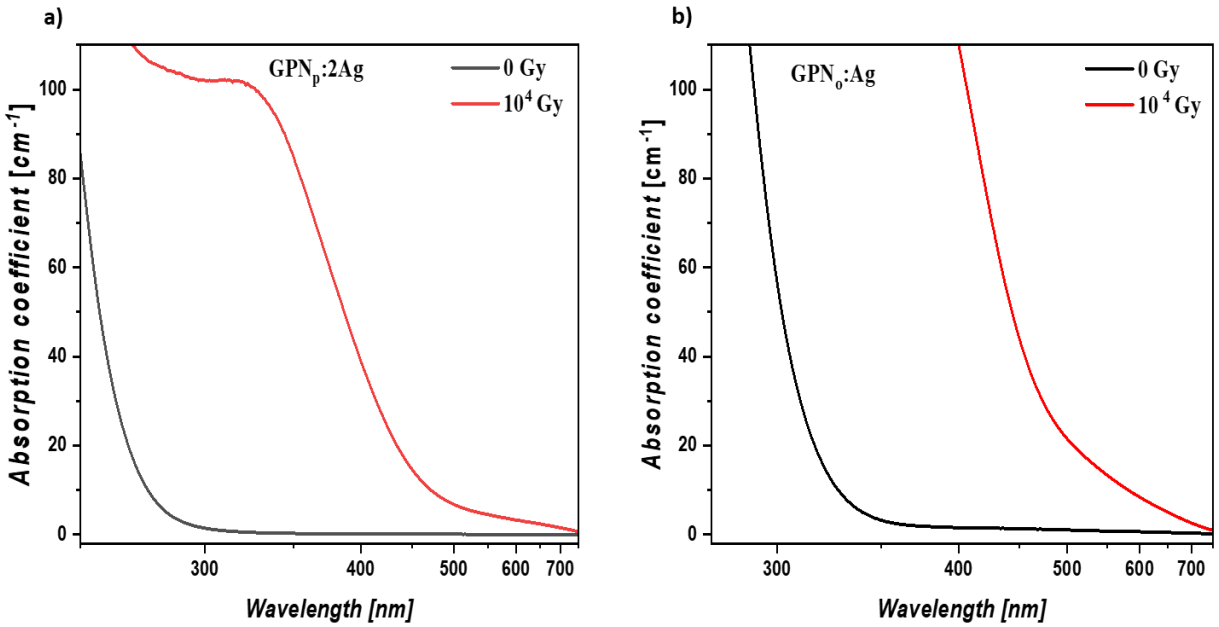

Figure 7:Absorption spectra of irradiated GPN_p :Ag (a) and GPN_o:Ag (b) glass at 10^4 Gy.

The photoluminescent property of the irradiated GPN_p:Ag and GPN_o:Ag has been performed at room temperature for two excitation wavelengths (320 nm and 405 nm) and is shown in Figure 8. For the excitation at 320 nm, the GPN_p:Ag irradiated at 10^4 Gy glass exhibits a broad emission band with the main contribution at 630 nm (Figure 8a black curve) characteristic of Ag^{2+} emission band and comparable to that of $PZnGa_{5.5}$:Ag_3 excited at 305 nm (Figure 4a red full curve). This finding confirms the presence of Ag^{2+} discussed in absorption and ESR spectroscopy. When the irradiation dose increase to 10^6 Gy, the contribution around 525 nm strongly increases (Figure 8a red curve) and reveals the existence of silver clusters as already mentioned for $PZnGa_{5.5}$:Ag_3 [9, 27, 37]. To better elucidate the presence of silver cluster, an excitation spectrum at a longer wavelength has been performed knowing that higher wavelength excitation (>380 nm) promotes preferentially the emission of silver cluster without exciting silver-colored centers. So, at 405 nm the emission band centered around 525 nm becomes dominant (Figure 8b) and can be compared to the emission band for excitation at 380 nm of $PZnGa_{5.5}$:Ag_3. The intensity of silver cluster emission increases with the dose traducing that the higher irradiation dose highly promotes the diffusion of silver species (Ag^0 and Ag^+) which combine to form silver clusters [38] as illustrated in equation (2). This phenomenon is in agreement with the weak ESR signal of Ag^0 at 10^6 Gy , which indicates that the majority of Ag^0 is consumed to form silver clusters. However, for GPN_o:Ag glass an intense emission assigned to the silver clusters can be seen already at 10^4 Gy with a maximum at 550 nm when excited at 320 nm or 405 nm which does not evolve with the irradiation dose (Figure 8c and 8d). The nature of silver clusters is here not dependent on the dose, even at 10^4 Gy, the majority of Ag^0 participates in the formation of clusters [18]. This phenomenon is also in accordance with the investigation of the femtosecond irradiation on sodium gallo phosphate glasses indicating that the orthophosphate compositions present the largest photosensitivity as previously reported [8].

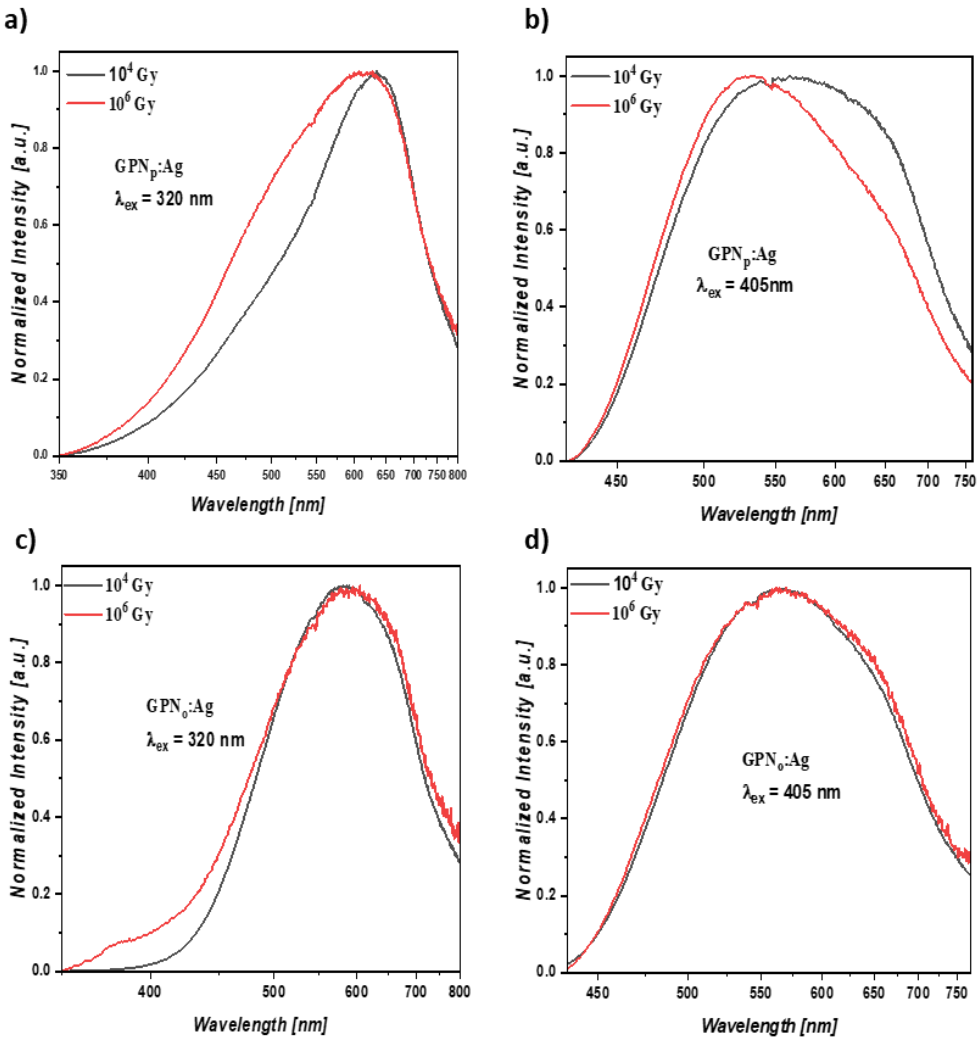

Figure 9 : Photoluminescence emission properties of the irradiated GPN_p :Ag and GPN_o :Ag glasses a&c) for 320nm excitation, and b&d) 405 nm excitation, at two different radiation doses (10^4 and 10^6 Gy)

3.6 Cathodoluminescence of $PZnGa_{5.5}:Ag_3$ and GPN_p:Ag glass

This section presents the in-situ luminescence measurement using cathodoluminescence and explores the direct excitation of the produced silver species. Pyrophosphate glass composition with the lowest sensitivity toward electron irradiation as compared to orthophosphate has been selected ($PZnGa_{5.5}:Ag_3$ and GPN_p) for monitoring in situ investigation. The measurement scheme consisted of irradiating the sample with the 2.5 MeV electron beam (used as excitation as well) and collecting the fluorescence emission of the glass instantaneously for a certain amount of time. The irradiation dose is directly related to irradiation time depending on the electron flux. This aims to follow instantly the process of silver cluster formation to study the silver ions chemistry under ionizing irradiation. The cathodoluminescence was conducted at a fixed current intensity and dose rate. The emission spectra were collected every 5 seconds or 30 seconds according to the current intensity. To dismiss the effect of an artifact originating from the measurement setup which presents an emission band around 420 nm when the current is equal to 5nA (low dose), the contribution of the artifact was subtracted from the signal, the resulting data are presented in Figure 9a and 9c. Figure 9a illustrates the emission spectra of silver containing $PZnGa_{5.5}:Ag_3$ glass irradiated with a 5 nA current and collected every 5

seconds. The first emission band collected at the beginning of the irradiation shows a slight broad band spanning the spectral range of 450 nm to 650 nm traducing the silver cluster's excitation by an electron beam. By increasing the irradiation time to 500 seconds, which corresponds to the irradiation dose of 4.5 kGy, one can observe a continuous raise of this contribution with a maximum around 500 nm. The same phenomena are observed in the GPN_p:Ag glass but with stronger emission (Figure 9c). This highly supports the abovementioned result as well as the photosensitivity of GPN_p:Ag compared to $PZnGa_{5.5}$:Ag_3. The cathodoluminescence performed at 5 µA current intensity on both GPN_p:Ag and $PZnGa_{5.5}$:Ag_3 displayed in Figures 9b and 9d respectively exhibit a broad emission band spanning the entire visible range with a peak around 500 nm which doesn't evolute in shape with the irradiation dose. The cathodoluminescence targeting the silver cluster emission illustrates their formation even at the early stage of irradiation.

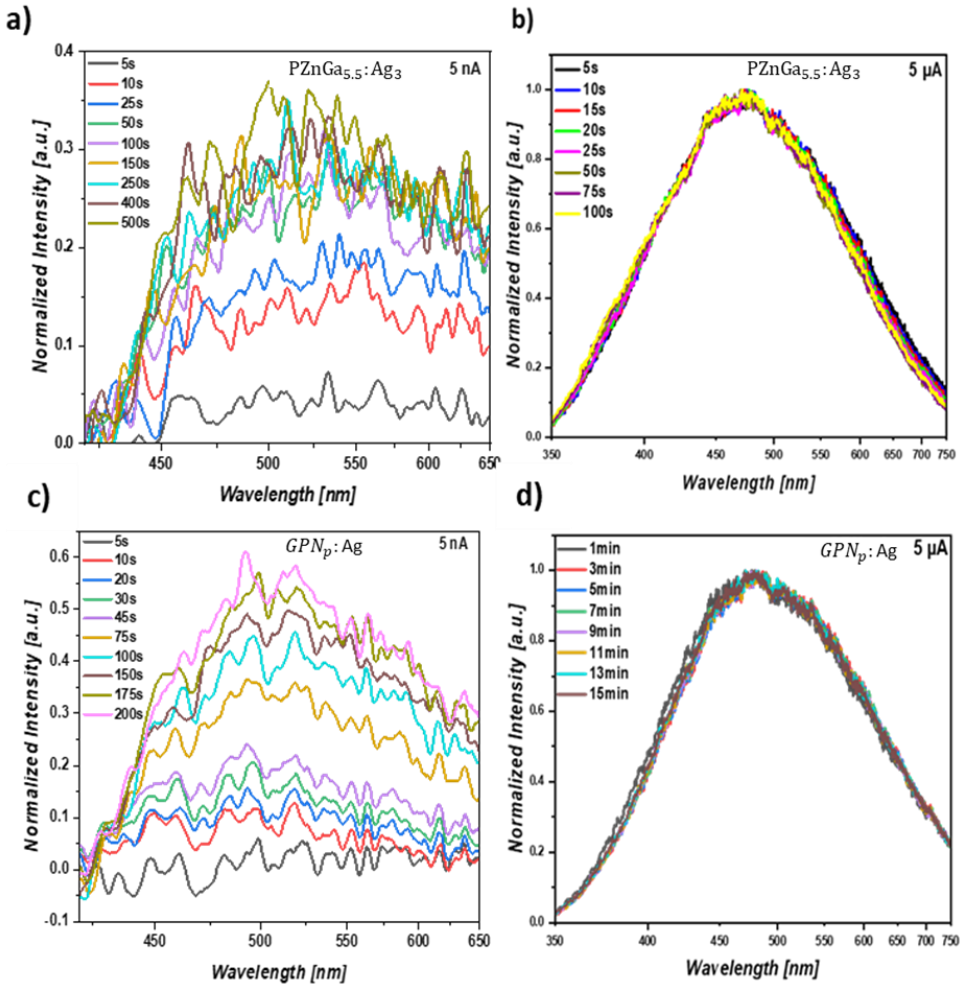

Figure 9: Catholuminescence of a,b) silver-doped $PZnGa_{5.5}$:Ag and c,d) GPN_p:Ag glasses

4 Conclusion

The impact of 2.5 MeV electron irradiation dose and silver in pyrophosphate and orthophosphate glasses was reported. The electron beam generated an electron-hole pair in the phosphate glasses which is initially captured by the phosphorus trapped center. In the presence of silver ions, this electron-hole pair is rather transferred to the silver ions to form Ag^0 atoms and Ag^{2+} ions. It has been then well illustrated that silver ions are the most susceptible species

to act as an electron-hole trapping center. The Ag^0 atoms formed following irradiation are rapidly associated with Ag^+ ions to form silver clusters. The occurrence of silver clusters has been observed by luminescence spectroscopy, but their detection in the ESR is limited by the experimental issue. Orthophosphate glass matrices are the most suitable for the formation of the hole and electron traps and the formation of the silver cluster in large quantities as compared to pyrophosphate. The cathodoluminescence allows collecting the progression of the silver cluster formation during the first step of irradiation and shows that the cluster is formed at the early stage of the irradiation. Finally, the luminescence properties induced by electron beam irradiation are quite comparable to the luminescence properties obtained after femtosecond direct laser writing. Thus, this finding allows making a connection between the nature of silver clusters formed during both electron beam and femtosecond laser irradiation. The process of silver clusters formation under an electron beam remains slow as compared to femtosecond laser. However, it allows not only following the electron and hole recombination in silver phosphate glasses but also brings some insight into the photochemistry process of silver under femtosecond laser irradiation, which is still under debate**.**

Declaration of Competing Interest

The authors declare that they have no known competing fi-nancial interests or personal relationships that could have appeared to influence the work reported in this paper.

Acknowledgments

This research has benefited financial support from French National Research Agency (ANR) ANR-19-CE08-0021-01, and from Région Nouvelle Aquitaine (project AAPR2020-2019-8193110). This project has received support funding from GPR IDEX Bordeaux and French National Research Agency (ANR) ANR- 21-PRRD-0001-01/ PDR- Stabilo.
Experiment done at LSI (Laboratoire des Solides Irradiés), Palaiseau, France and supported by the French Network EMIR.

References

[1] J. E. MARION et M. J. WEBER, « Phosphate laser glasses », *Phosphate Laser Glas.*, vol. 28, nº 1, p. 271-287, 1991.
[2] A. Henglein, « Non-metallic silver clusters in aqueous solution: stabilization and chemical reactions », *Chem. Phys. Lett.*, vol. 154, nº 5, p. 473-476, févr. 1989, doi: 10.1016/0009-2614(89)87134-9.
[3] B. G. Ershov, E. Janata, et A. Henglein, « Growth of silver particles in aqueous solution: long-lived "magic" clusters and ionic strength effects », *J. Phys. Chem.*, vol. 97, nº 2, p. 339-343, janv. 1993, doi: 10.1021/j100104a013.
[4] N. Marquestaut, Y. Petit, A. Royon, P. Mounaix, T. Cardinal, et L. Canioni, « Three-Dimensional Silver Nanoparticle Formation Using Femtosecond Laser Irradiation in Phosphate Glasses: Analogy with Photography », *Adv. Funct. Mater.*, vol. 24, nº 37, p. 5824-5832, 2014, doi: 10.1002/adfm.201401103.
[5] R. Espiau de Lamaestre, H. Béa, H. Bernas, J. Belloni, et J. L. Marignier, « Irradiation-induced Ag nanocluster nucleation in silicate glasses: Analogy with photography », *Phys. Rev. B*, vol. 76, nº 20, p. 205431, nov. 2007, doi: 10.1103/PhysRevB.76.205431.
[6] A. Royon, K. Bourhis , M. Bellec , G. Papon , B. Bousquet , Y. Deshayes , T. Cardinal , and L. Canioni., « Silver Clusters Embedded in Glass as a Perennial High Capacity Optical Recording Medium », *Adv. Mater.*, vol. 22, nº 46, p. 5282-5286, 2010, doi: 10.1002/adma.201002413.
[7] M. Bellec, Arnaud Royon, K. Bourhis, J. Choi, B. Bousquet, M. Treguer, T. Cardinal, J-J. Videau, M. Richardson and L. Canioni « 3D Patterning at the Nanoscale of Fluorescent Emitters in Glass », *J. Phys. Chem. C*, vol. 114, nº 37, p. 15584-15588, sept. 2010, doi: 10.1021/jp104049e.
[8] T. Guérineau, L. Loi, Y. Petit, S. Danto, A. Fargues, L. Canioni, and T. Cardinal, « Structural influence on the femtosecond laser ability to create fluorescent patterns in silver-containing sodium-gallium phosphate glasses », *Opt. Mater. Express*, vol. 8, nº 12, p. 3748-3760, déc. 2018, doi: 10.1364/OME.8.003748.
[9] K. Bourhis, A. Royon, M. Bellec, J. Choi, A. Fargues, M. Treguer, J-J. Videau, D. Talaga, M. Richardson, T. Cardinal, L. Canioni. « Femtosecond laser structuring and optical properties of a silver and zinc phosphate glass », *J. Non-Cryst. Solids*, vol. 356, nº 44, p. 2658-2665, oct. 2010, doi: 10.1016/j.jnoncrysol.2010.03.033.
[10] G. Papon, Y. Petit, N. Marquestaut, A. Royon, M. Dussauze, V. Rodriguez, T. Cardinal, L. Canioni « Fluorescence and second-harmonic generation correlative microscopy to probe space charge separation and silver cluster stabilization during direct laser writing in a tailored silver-containing glass », *Opt. Mater. Express*, vol. 3, nº 11, p. 1855-1861, nov. 2013, doi: 10.1364/OME.3.001855.
[11] G. Papon, N. Marquestaut, Y. Petit, A. Royon, M. Dussauze, V. Rodriguez, T. Cardinal, L. Canioni « Femtosecond single-beam direct laser poling of stable and efficient second-order nonlinear optical properties in glass », *J. Appl. Phys.*, vol. 115, nº 11, p. 113103, mars 2014, doi: 10.1063/1.4869058.
[12] L. Canioni, M. Bellec, A. Royon, B. Bousquet, et T. Cardinal, « Three-dimensional optical data storage using third-harmonic generation in silver zinc phosphate glass », *Opt. Lett.*, vol. 33, nº 4, p. 360-362, févr. 2008, doi: 10.1364/OL.33.000360.
[13] G.Y. Shakhgildyan, A.S. Lipatiev, M.P. Vetchinnikov, V.V. Popova, S.V. Lotarev, N.V. Golubev, E.S. Ignat'eva, M.M. Presniakov, V.N. Sigaev « One-step micro-modification of optical properties in silver-doped zinc phosphate glasses by femtosecond direct laser writing », *J. Non-Cryst. Solids*, vol. 481, p. 634-642, févr. 2018, doi: 10.1016/j.jnoncrysol.2017.12.011.

[14] A. A. Khalil, J-P. Bérubé, S. Danto, J-C. Desmoulin, T. Cardinal, Y. Petit, R. Vallée & L. Canioni « Direct laser writing of a new type of waveguides in silver containing glasses », *Sci. Rep.*, vol. 7, nº 1, Art. nº 1, sept. 2017, doi: 10.1038/s41598-017-11550-0.
[15] A. A. Khalil, J-P. Bérubé, S. Danto, T. Cardinal, Y. Petit, R. Vallée & L. Canioni « Comparative study between the standard type I and the type A femtosecond laser induced refractive index change in silver containing glasses », *Opt. Mater. Express*, vol. 9, nº 6, p. 2640-2651, juin 2019, doi: 10.1364/OME.9.002640.
[16] R. K. Brow, R. J. Kirkpatrick, et G. L. Turner, « Nature of Alumina in Phosphate Glass: II, Structure of Sodium Alurninophosphate Glass », *J. Am. Ceram. Soc.*, vol. 76, nº 4, p. 919-928, 1993, doi: 10.1111/j.1151-2916.1993.tb05316.x.
[17] R. K. Brow, « Review: the structure of simple phosphate glasses », *J. Non-Cryst. Solids*, vol. 263-264, p. 1-28, mars 2000, doi: 10.1016/S0022-3093(99)00620-1.
[18] T. Guérineau, F. Cova, Y. Petit, A. A. Khalil, A. Fargues, M. Dussauze, S. Danto, A. Vedda, L. Canioni, T. Cardinal « Silver centers luminescence in phosphate glasses subjected to X-Rays or combined X-rays and femtosecond laser exposure », *Int. J. Appl. Glass Sci.*, vol. 11, nº 1, p. 15-26, 2020, doi: 10.1111/ijag.13957.
[19] R. Yokota et H. Imagawa, « ESR Studies of Radiophotoluminescent Centers in Silver-Activated Phosphate Glass », *J. Phys. Soc. Jpn.*, vol. 20, nº 8, p. 1537-1538, 1965, doi: 10.1143/JPSJ.20.1537.
[20] Y. Miyamoto *et al.*, « Radiophotoluminescence from silver-doped phosphate glass », *Radiat. Meas.*, vol. 46, nº 12, p. 1480-1483, déc. 2011, doi: 10.1016/j.radmeas.2011.05.048.
[21] H. Tanaka *et al.*, « Radiophotoluminescence properties of Ag-doped phosphate glasses », *Radiat. Meas.*, vol. 94, p. 73-77, nov. 2016, doi: 10.1016/j.radmeas.2016.09.002.
[22] R. Yokota et H. Imagawa, « Radiophotoluminescent Centers in Silver-Activated Phosphate Glass », *J. Phys. Soc. Jpn.*, vol. 23, nº 5, p. 1038-1048, nov. 1967, doi: 10.1143/JPSJ.23.1038.
[23] Y. Miyamoto, Y. Takei, H. Nanto, T. Kurobori, A. Konnai, T. Yanagida, A. Yoshikawa, Y. Shimotsuma, M. Sakakura, K. Miura, K. Hirao, Y. Nagashima, T. Yamamoto « Emission and excitation mechanism of radiophotoluminescence in Ag+-activated phosphate glass », *Nucl. Instrum. Methods Phys. Res. Sect. Accel. Spectrometers Detect. Assoc. Equip.*, vol. 619, nº 1, p. 71-74, juill. 2010, doi: 10.1016/j.nima.2010.02.076.
[24] L. B. Fletcher, J. J. Witcher, N. Troy, S. T. Reis, R. K. Brow, et D. M. Krol, « Direct femtosecond laser waveguide writing inside zinc phosphate glass », *Opt. Express*, vol. 19, nº 9, p. 7929-7936, avr. 2011, doi: 10.1364/OE.19.007929.
[25] L. B. Fletcher *et al.*, « Femtosecond laser writing of waveguides in zinc phosphate glasses [Invited] », *Opt. Mater. Express*, vol. 1, nº 5, p. 845-855, sept. 2011, doi: 10.1364/OME.1.000845.
[26] I. Belharouak, « Luminescence de l'argent dans les phosphates », phdthesis, Université Sciences et Technologies - Bordeaux I, 1999. Consulté le: 25 juin 2022. [En ligne]. Disponible sur: https://tel.archives-ouvertes.fr/tel-00972640
[27] Y. Petit, S. Danto, T. Guérineau, A. A. Khalil, A. Le Camus, E. Fargin, G. Duchateau, J-P. Bérubé, R. Vallée, Y. Messaddeq, T. Cardinal and L. Canioni « On the femtosecond laser-induced photochemistry in silver-containing oxide glasses: mechanisms, related optical and physico-chemical properties, and technological applications », *Adv. Opt. Technol.*, vol. 7, nº 5, p. 291-309, oct. 2018, doi: 10.1515/aot-2018-0037.
[28] S. Danto, F. Désévédavy, Y. Petit, J-C. Desmoulin, A. A. Khalil, C. Strutynski, M. Dussauze, F. Smektala, T. Cardinal, and L. Canioni « Photowritable Silver-Containing

Phosphate Glass Ribbon Fibers », *Adv. Opt. Mater.*, vol. 4, nº 1, p. 162-168, 2016, doi: 10.1002/adom.201500459.
[29] P. Ebeling, D. Ehrt, et M. Friedrich, « X-ray induced effects in phosphate glasses », *Opt. Mater.*, vol. 20, nº 2, p. 101-111, sept. 2002, doi: 10.1016/S0925-3467(02)00052-6.
[30] V. Pukhkaya, F. Trompier, et N. Ollier, « New insights on P-related paramagnetic point defects in irradiated phosphate glasses: Impact of glass network type and irradiation dose », *J. Appl. Phys.*, vol. 116, nº 12, p. 123517, sept. 2014, doi: 10.1063/1.4896876.
[31] D. L. Griscom, E. J. Friebele, K. J. Long, et J. W. Fleming, « Fundamental defect centers in glass: Electron spin resonance and optical absorption studies of irradiated phosphorus-doped silica glass and optical fibers », *J. Appl. Phys.*, vol. 54, nº 7, p. 3743-3762, juill. 1983, doi: 10.1063/1.332591.
[32] H. Kawamoto, H. Tanaka, M. Koshimizu, Y. Fujimoto, et K. Asai, « Hole transfer in Ag-doped phosphate glasses having different cations elucidated by measuring variation of electron spin resonance spectra and photoluminescence spectra over time », *Nucl. Instrum. Methods Phys. Res. Sect. B Beam Interact. Mater. At.*, vol. 479, p. 137-142, sept. 2020, doi: 10.1016/j.nimb.2020.06.014.
[33] Jacek. Michalik et Larry. Kevan, « Paramagnetic silver clusters in Ag-NaA zeolite: electron spin resonance and diffuse reflectance spectroscopic studies », *J. Am. Chem. Soc.*, vol. 108, nº 15, p. 4247-4253, juill. 1986, doi: 10.1021/ja00275a001.
[34] G. Okada, T. Kojima, J. Ushizawa, N. Kawaguchi, et T. Yanagida, « Radio-photoluminescence observed in non-doped Mg2SiO4 single crystal », *Curr. Appl. Phys.*, vol. 17, nº 3, p. 422-426, mars 2017, doi: 10.1016/j.cap.2017.01.004.
[35] H. W. Etzel et J. H. Schulman, « Silver-Activated Alkali Halides », *J. Chem. Phys.*, vol. 22, nº 9, p. 1549-1554, sept. 1954, doi: 10.1063/1.1740455.
[36] D. Möncke, S. Reibstein, D. Schumacher, et L. Wondraczek, « Irradiation-induced defects in ionic sulfophosphate glasses », *J. Non-Cryst. Solids*, vol. 383, p. 33-37, janv. 2014, doi: 10.1016/j.jnoncrysol.2013.04.029.
[37] K. Bourhis, A. Royon, G. Papon, M. Bellec, Y. Petit, L. Canioni, M. Dussauze, V. Rodriguez, L. Binet, D. Caurant, M. Treguer, J-J. Videau, T. Cardinal « Formation and thermo-assisted stabilization of luminescent silver clusters in photosensitive glasses », *Mater. Res. Bull.*, vol. 48, nº 4, p. 1637-1644, avr. 2013, doi: 10.1016/j.materresbull.2013.01.003.
[38] M. E. Archidi, M. Haddad, A. Nadiri, F. Benyaïch, et R. Berger, « Defect centers in X-irradiated alkali phosphate glasses: EPR studies », *Nucl. Instrum. Methods Phys. Res. Sect. B Beam Interact. Mater. At.*, vol. 116, nº 1, p. 145-149, août 1996, doi: 10.1016/0168-583X(96)00026-2.